

## CHAPTER 4 RESULTS

### 4.1 Trends of Sea Level in the Gulf of Thailand and the South China Sea

The Intergovernmental Panel on Climate Change (IPCC) Report estimates that the global sea level rise was approximately 1.7 - 1.8 mm/yr over the past century (IPCC, 2007) based on tide gauge stations around the world and global climate models. The National Oceanic and Atmospheric Administration (NOAA) reported the sea level will rise in some regions (NOAA, 2010), see Figure 4.1. This report reveals the online trends of sea level in the Gulf of Thailand (GoT) and the South China Sea (SCS) rising for all tide gauge stations except at Ko Lak station. Linear regression to the sea level in the SCS indicates that mean sea level has a rise rate of 11.3 mm/yr during 1993 - 2000 and a fall rate of 11.8 mm/yr during 2001 - 2005 (Cheng and Qi, 2007).



Figure 4.1 The sea level in the Gulf of Thailand and the South China Sea (NOAA, 2010).

In this section, the sea level observations are obtained from Hydrographic Department, Marine Department and the Permanent Service for Mean Sea Level (PSMSL). The annual sea level trends from 23 tide gauge stations, as Figure 4.2, in the GoT and the SCS are investigated using two methods: least square linear regression and periodic cubic spline approximation.

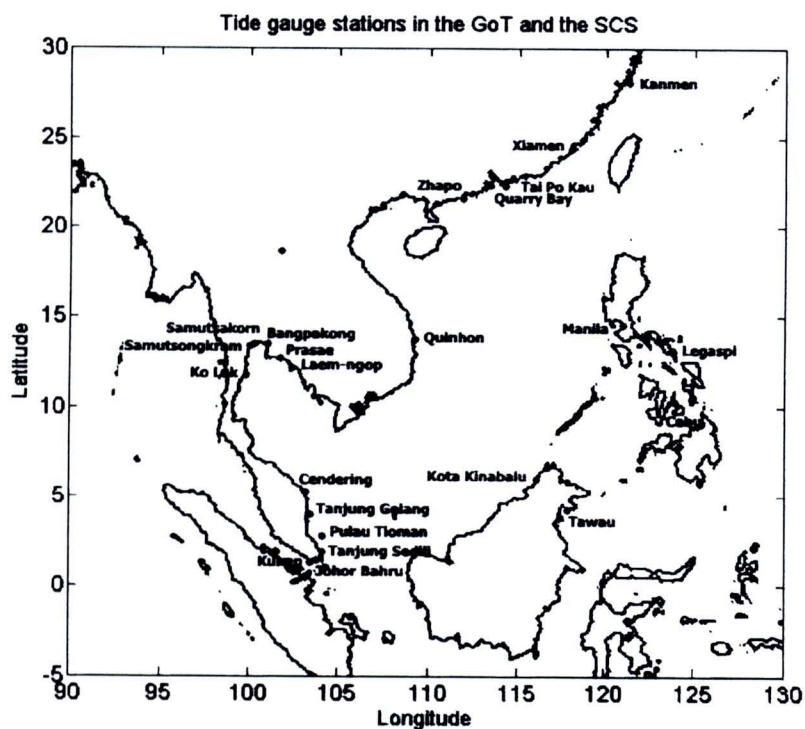
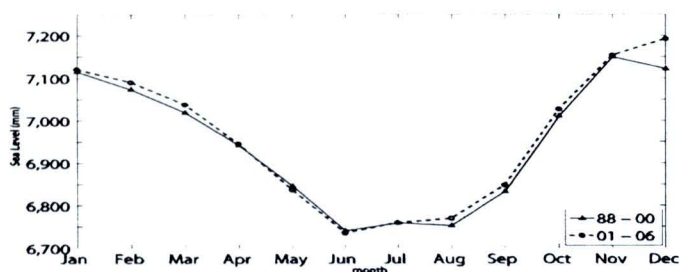
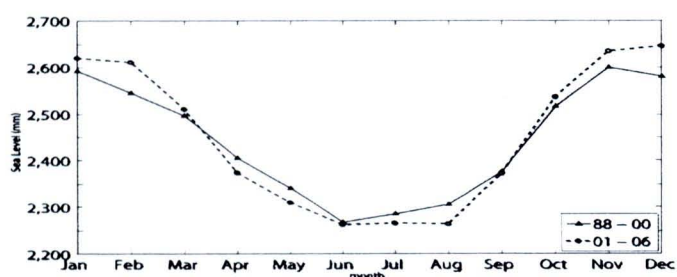


**Figure 4.2** The 23 tide gauge stations in the Gulf of Thailand and the South China Sea.

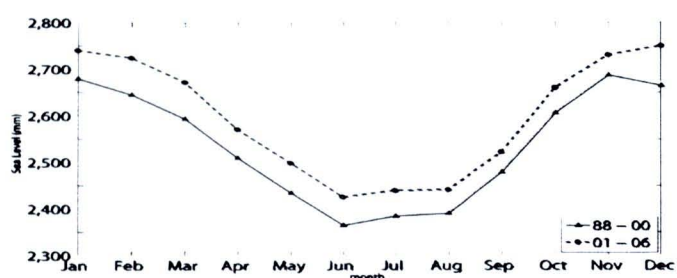
Firstly, the monthly sea level in the GoT are considered by separating the time domain before and after the year 2000, that is the periods of 1988 - 2000 and 2001 - 2006 for comparison. The data sets of monthly sea level from Bangpakong station, Samutsakorn station, Samutsongkram station, Ko Lak station, Laem-ngop station and Prasae station are investigated. Normally, the sea level would fall in the summer season and would increase in rainy season, see Figure 4.3. Results show that the monthly sea level in the period 2001 - 2006 is higher than the past period 1988 - 2000 for each station but except Laem-ngop station. At Laem-ngop station, the sea level on April - September in the period 2001 - 2006 is lower than the past period 1988 - 2000.



(a)



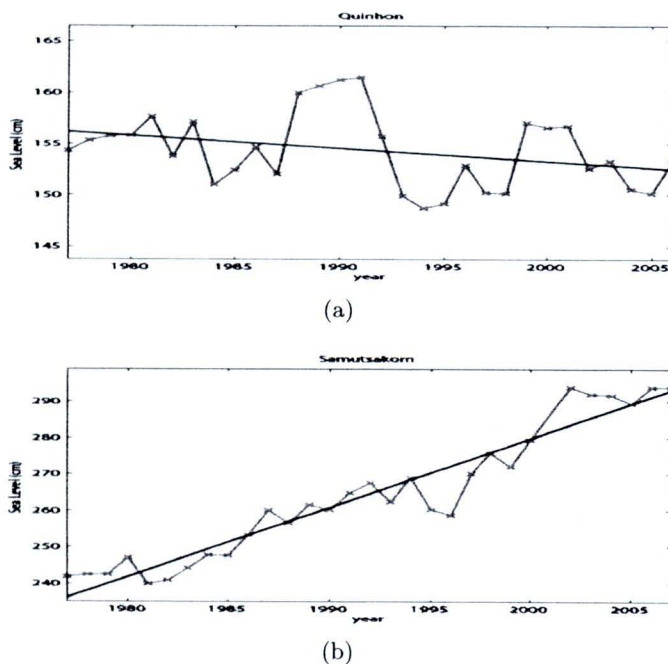
(b)



(c)

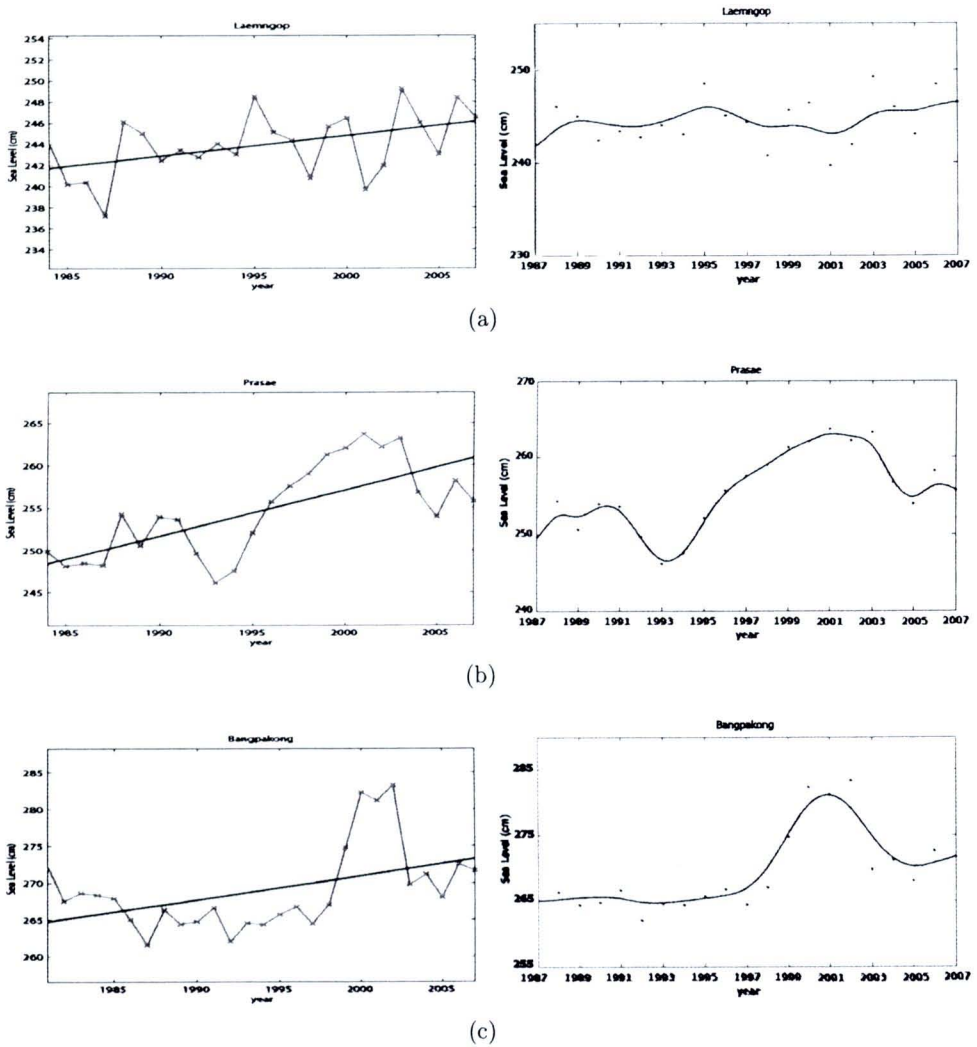
**Figure 4.3** The monthly sea level in the Gulf of Thailand during 1988 - 2000 (solid line) and 2001 - 2006 (dash line) at: (a) Ko Lak station, (b) Laem-ngop station and (c) Prasae station.

The trends of sea level from tide gauge stations in the GoT and the SCS using least square linear regression and periodic cubic spline approximation methods are shown at selected stations, see Figures 4.5 - 4.7. The least square linear regression is used to investigate the trends and rates of annual sea level changes during 1977 - 2007 and the periodic cubic spline approximation is used to find the general trends of annual sea level in the GoT and the SCS during the year 1987 - 2007 and 1959 - 2006, respectively. The results show that the annual sea level have been increased, except at Quinhon station the annual mean sea level fall with rate of 1.26 mm/yr for the year 1977 - 2006 (Figure 4.4(a)). The annual sea level has a highest rate of rising 19.02 mm/yr during 1977 - 2007 at Samutsakorn station (Figure 4.4(b)).



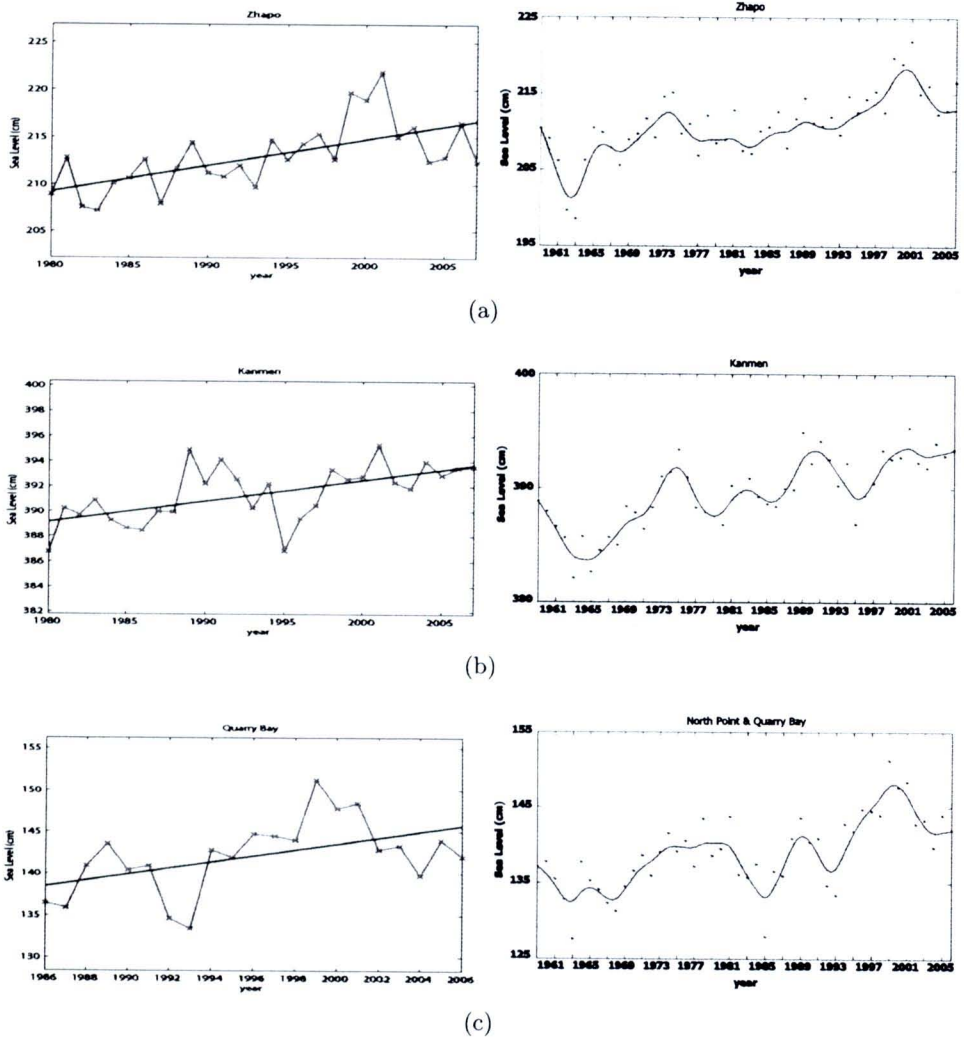
**Figure 4.4** The lowest and highest trends of annual sea level at: (a) Quinhon station and (b) Samutsakorn station.

Figure 4.5 shows the trends of annual sea level at Laem-ngop station, Prasae station and Bangpakong station in the GoT. The trends of sea level have been risen in the GoT. At Laem-ngop station, the trend of sea level is continuous increasing during 1987 - 2007. The trend of sea level is falling in the year 1991 - 1993 and is immediately rising during 1994 - 2003 at Prasae station. At Bangpakong station, the trend of sea level is stand level during 1987 - 1997, but it is increasing and peak in the year 2001.



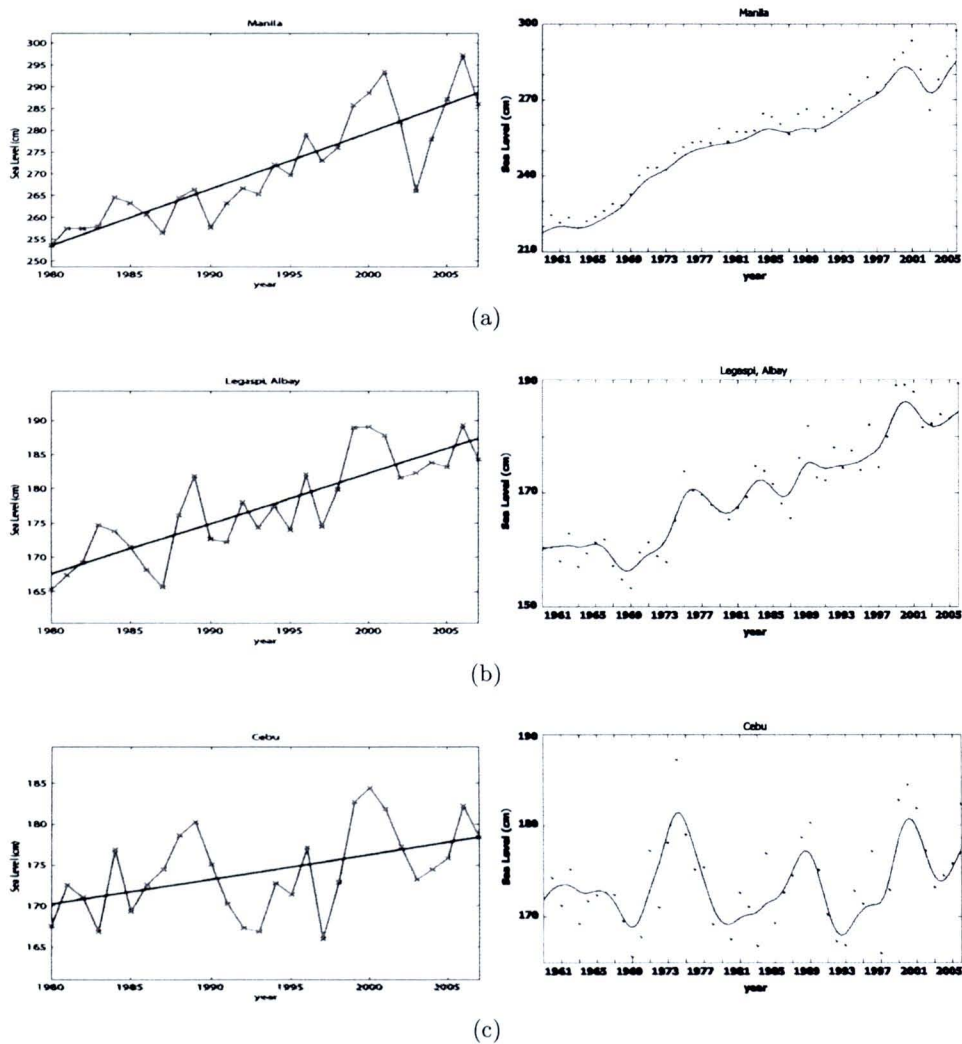
**Figure 4.5** The trends of annual sea level using least square linear regression (left panel) and periodic cubic spline approximation (right panel) at: (a) Laem-ngop station, (b) Prasae station and (c) Bangpakong station.

Figure 4.6 reveals the trends of sea level at Zhapo station, Kanmen station and Quarry Bay station in China. These trends are rising during 1960 - 2006. There are peaks in year 2001 at Zhapo station and Kanmen station and in year 1999 at Quarry Bay station.



**Figure 4.6** Same as Figure 4.5 except for: (a) Zhapo station, (b) Kanmen station and (c) Quarry Bay station.

Figure 4.7 shows the trends of sea level at Manila, S. Harbor station, Legaspi, Albay station and Cebu station in the Philippines. The trend of sea level is highest rising with a rate of 13.00 mm/yr at Manila, S. Harbor station in the Philippines. The trends of sea level at Manila, S. Harbor station and Legaspi, Albay station are really rising during 1960 - 2006. At Cebu station, the trend of sea level is oscillatory increasing with the peak in year 1973, 1989 and 2000.



**Figure 4.7** Same as Figure 4.5 except for: (a) Manila, S. Harbor station, (b) Legaspi, Albay station and (c) Cebu station.

Rates of sea level changes at all stations in the GoT and the SCS are shown in Table 4.1. The two highest rates of sea level rise of 19.02 and 15.36 mm/yr are found at Samutsakorn station and Samutsongkram station in the GoT, respectively. The rates of rising along the coast of the GoT are of 0.81 - 19.02 mm/yr. The rates of sea level rise are 1.07 - 3.20 mm/yr along the coast of Malaysia. The rates of sea level rise are 1.69 - 2.77 mm/yr along the coast of China. The rates of sea level rise are 3.02 - 13.00 mm/yr in the Philippines, especially at Manila, S. Harbor station the high rising rates of 13 mm/yr.

**Table 4.1** The rates of sea level rise in the Gulf of Thailand and the South China Sea

Station Name	Period	Rate (mm/yr)
Samutsongkram	1980 - 2007	15.36
Prasae	1984 - 2007	5.42
Laem-ngop	1984 - 2007	1.92
Bangpakong	1981 - 2007	3.27
Ko Lak	1985 - 2007	0.81
Samutsakorn	1977 - 2007	19.02
Zhapo	1980 - 2007	2.77
Xiamen	1980 - 2004	1.69
Kanmen	1980 - 2007	2.76
Tai Po Kau, Tolo Harbour	1980 - 2006	5.27
Quarry Bay	1986 - 2006	3.63
Kukup	1980 - 2007	1.17
Johor Bahru	1984 - 2006	1.87
Tanjung Sedili	1987 - 2006	1.28
Pulau Tioman	1986 - 2006	1.07
Tanjung Gelang	1984 - 2006	2.11
Cendering	1985 - 2006	2.30
Kota Kinabalu	1988 - 2006	3.20
Tawau	1988 - 2006	1.81
Quinhon	1977 - 2006	-1.26
Manila, S. Harbor	1980 - 2007	13.00
Legaspi, Albay	1980 - 2007	7.33
Cebu	1980 - 2007	3.02

This result indicates the trends of sea level from tide gauge stations had been increased in the GoT with rising rates of 0.81 - 19.02 mm/yr and the SCS with rising rates of 1.07 - 13.00 mm/yr, except for Quinhon station the sea level had been fallen with rate of 1.26 mm/yr. The results agree with many researches (Yanagi and Akaki, 1994; Wong, et al., 2003; IPCC, 2007; NOAA, 2010) that sea level rise in some stations but not agree with some reports (Vongvisessomjai, 2006; Niemnil and Trisirisatayawong, 2006; NOAA, 2010) especially at Ko Lak station.

## 4.2 Empirical Orthogonal Functions

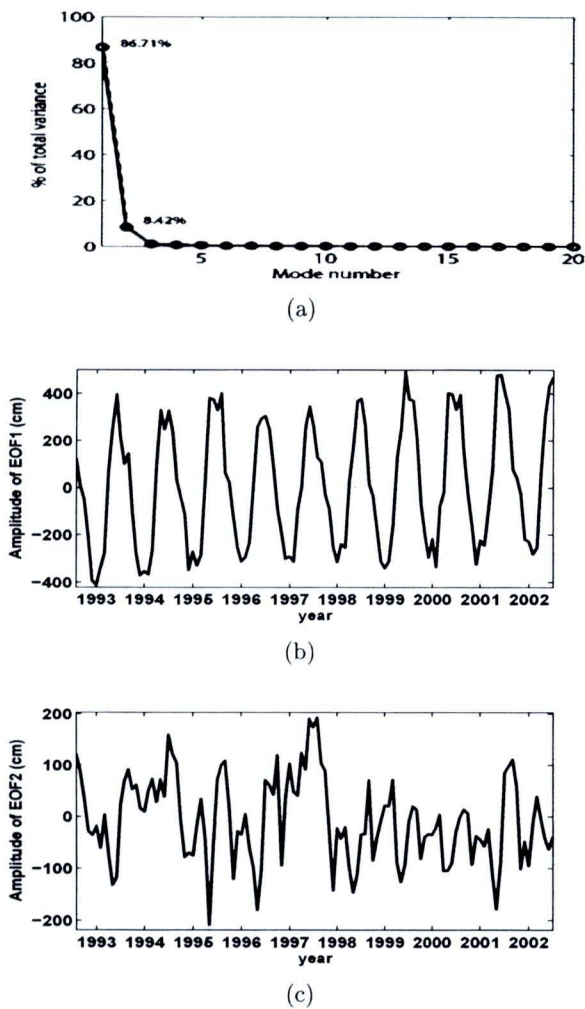
The EOF analysis is used to identify the dominant modes of the observation and results from numerical ocean models. There are many grided data types for analysis in the GoT and the SCS during February 1993 to January 2003 such as SSHA from TOPEX/ERS, SSHs from OCCAM with resolutions of  $1/4^\circ$  and  $1/12^\circ$  and SSH from POM.

### 4.2.1 EOF of SSHA from TOPEX/ERS Altimeter

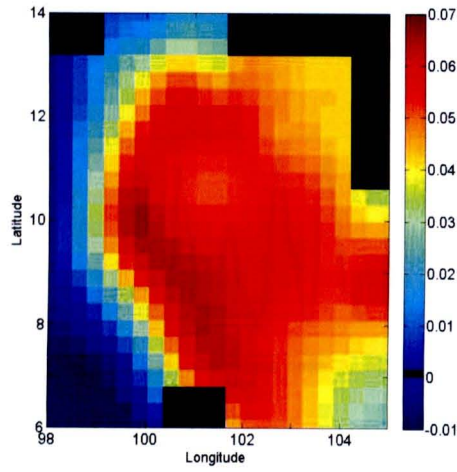
The SSHA from TOPEX/ERS during February 1993 to January 2003 are investigated the dominant mode in the GoT and the SCS. The EOF analysis is done on irregular  $1/3^\circ$  grid spacing. The period 120 months of SSHA are used for computing the covariance matrix. The data grids in space are  $23 \times 26$  and  $56 \times 79$  for each time in the GoT and the SCS regions, respectively.

Figure 4.8 reveals the percentages of total variance and their principal components of SSHA in the GoT. The first two modes explain 95.13% of total variance with mode 1 and 2 containing 86.71% and 8.42% of the total variance, respectively. Figure 4.9 shows the first two EOF modes of spatial patterns (more details about missing data in appendix) associated with the principal components of SSHA. The 1<sup>st</sup> mode represents the feature near the coast of the GoT, especially in the southern coast of the GoT. The 2<sup>nd</sup> mode shows variations in the western and central of the GoT.

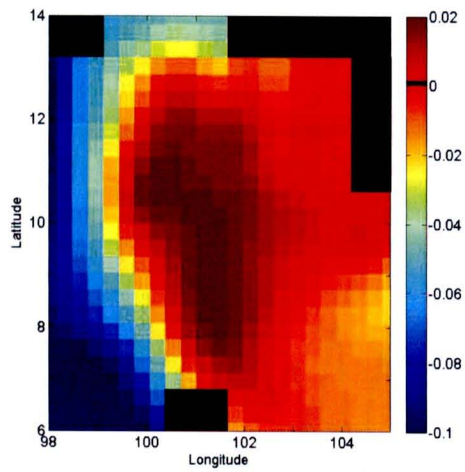
Figures 4.10 - 4.11 show the percentages of total variance, principal components and their spatial patterns of SSHA in the SCS. The first three modes account 71.42% of total variance with mode 1, 2 and 3 explaining 44.22%, 20.08% and 7.12% of the total variance, respectively. The 1<sup>st</sup> mode shows variations near the northern and southern coast of Veit Nam and along the coast of China. The 2<sup>nd</sup> mode represents the feature in the northern and eastern of the SCS and other locations in the Philippines. The 3<sup>rd</sup> mode shows the variations in the northern and central of the SCS.



**Figure 4.8** EOF of SSHA from TOPEX/ERS altimeter during Feb 1993 to Jan 2003 in the GoT: (a) % of the total variance, (b) the principal components of SSHA mode 1 and (c) the principal components of SSHA mode 2.

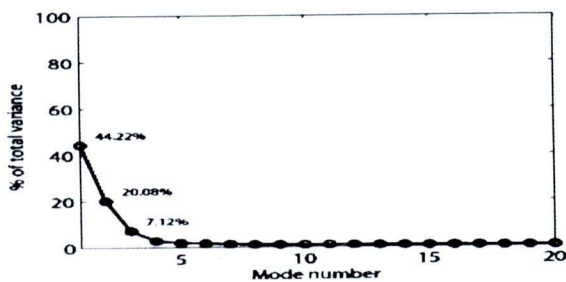


(a)

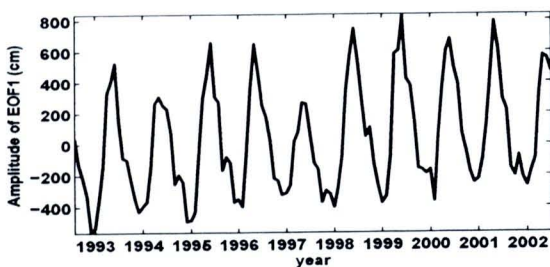


(b)

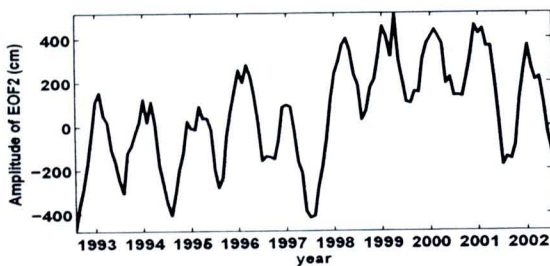
**Figure 4.9** The spatial patterns associated with their principal components of SSHA in the GoT for: (a) mode 1 and (b) mode 2.



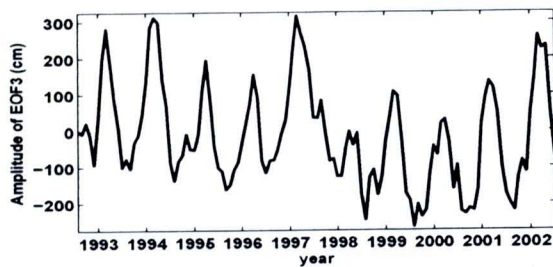
(a)



(b)



(c)



(d)

**Figure 4.10** EOF of SSHA from TOPEX/ERS altimeter during Feb 1993 to Jan 2003 in the SCS: (a) % of the total variance, (b) the principal components of SSHA mode 1, (c) the principal components of SSHA mode 2 and (d) the principal components of SSHA mode 3.

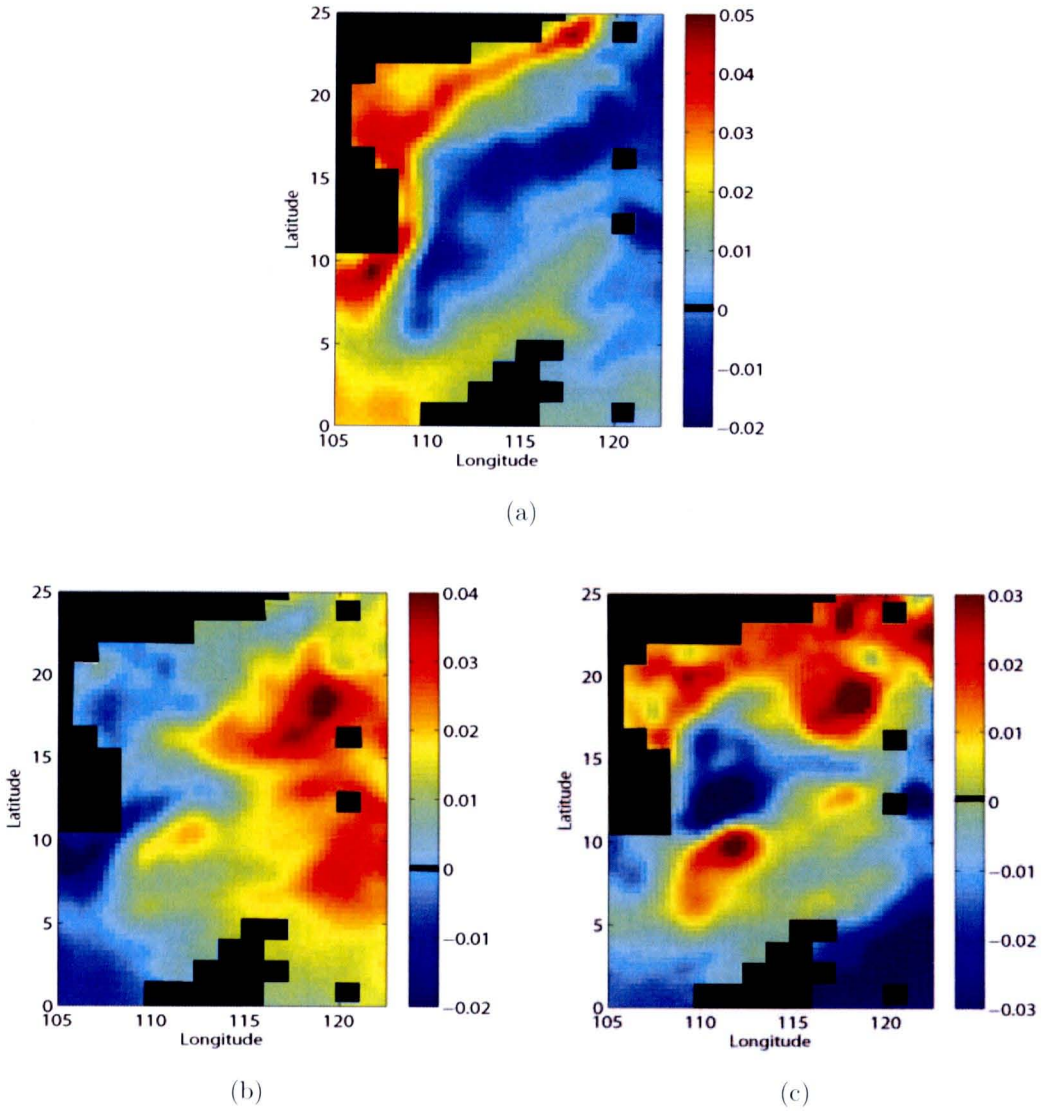


**Figure 4.11** The spatial patterns associated with their principal components of SSHA in the SCS for: (a) mode 1, (b) mode 2 and (c) mode 3.

#### 4.2.2 EOF of SSH from OCCAM with a resolution of $1/4^\circ$

The SSHs from OCCAM with a resolution of  $1/4^\circ$  are  $29 \times 33$  and  $73 \times 101$  for each time series in the GoT and the SCS regions, respectively. There are 120 months during February 1993 to January 2003.

Figure 4.12 shows the percentage of total variance and principal components of SSHs in the GoT. The first two modes account explaining 98.27% of total variance with mode 1 and 2 explaining 90.70% and 7.57% of the total variance, respectively. Figure 4.13 reveals the two highest spatial patterns associated with their principal components of SSH in the GoT. The 1<sup>st</sup> mode represents the annual variations in the GoT. The 2<sup>nd</sup> mode shows the variations in the central and southern of the GoT.

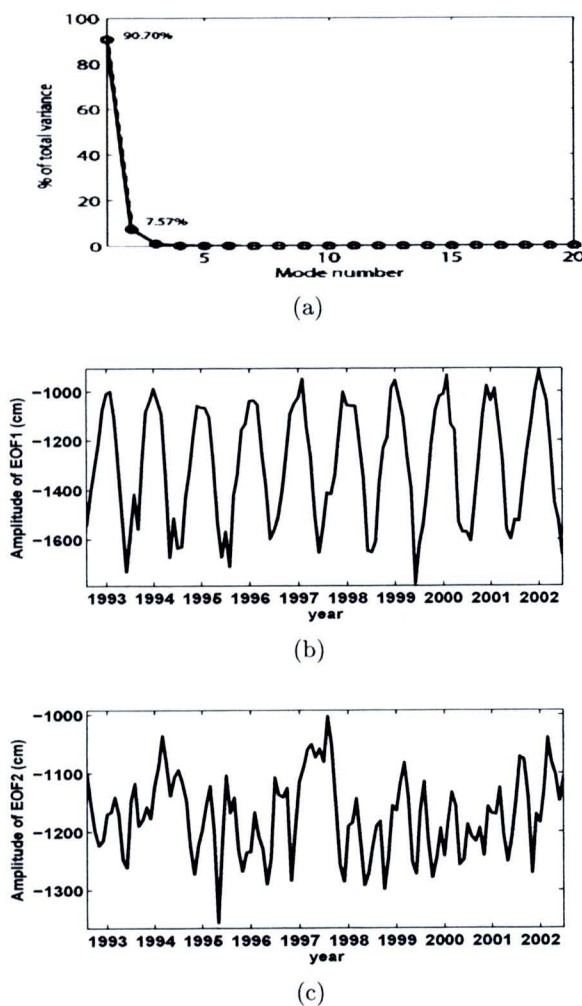
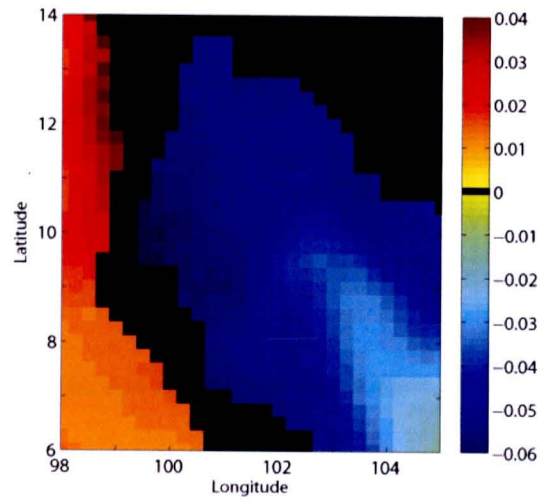
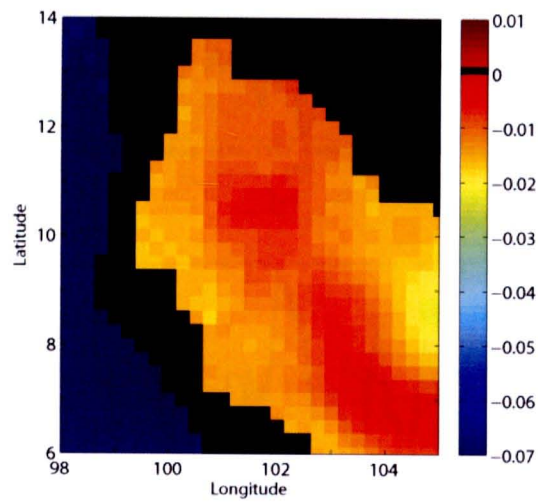


**Figure 4.12** EOF of SSH from OCCAM with a resolution of  $1/4^\circ$  during Feb 1993 to Jan 2003 in the GoT: (a) % of the total variance, (b) the principal components of SSH mode 1 and (c) the principal components of SSH mode 2.



(a)



(b)

**Figure 4.13** The spatial patterns associated with their principal components of SSH in the GoT for: (a) mode 1 and (b) mode 2.

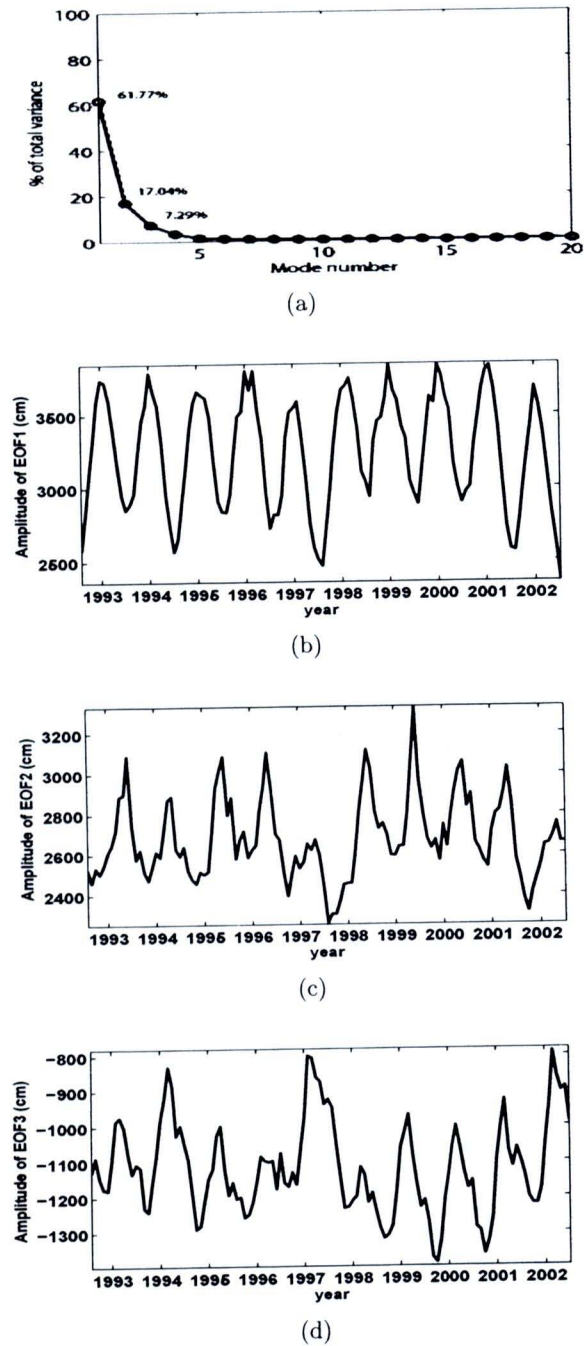
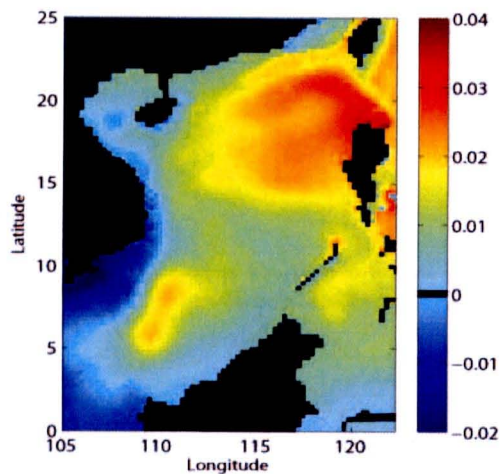
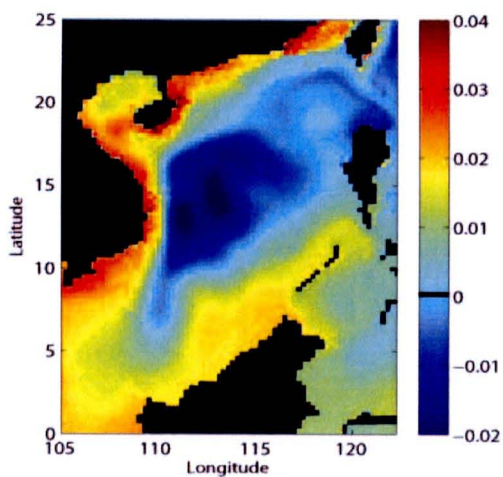


**Figure 4.14** EOF of SSH from OCCAM with a resolution of  $1/4^\circ$  during Feb 1993 to Jan 2003 in the SCS: (a) % of the total variance, (b) the principal components of SSH mode 1, (c) the principal components of SSH mode 2 and (d) the principal components of SSH mode 3.

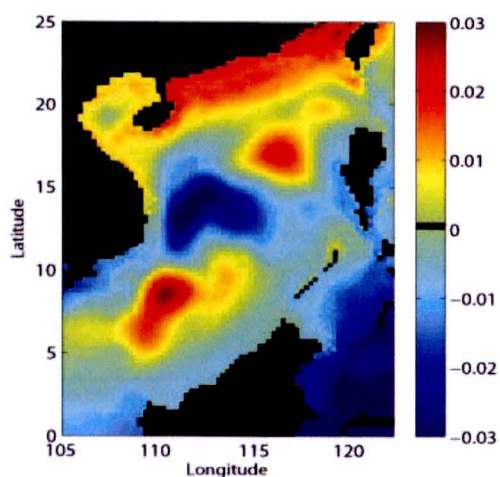
Figure 4.14 reveals the first three modes of EOF in the SCS region which explain 86.10% of total variance of SSH with mode 1, 2 and 3 containing 61.77%, 17.04% and 7.29% of total variance, respectively. Figure 4.15 shows the first three spatial patterns associated with their principal components of SSH in the SCS. The 1<sup>st</sup> mode shows the features in the northern and southern of the SCS and along the coast of the Philippines. The 2<sup>nd</sup> mode represents variations along the coast of China and Viet Nam and in the southern of the SCS. The 3<sup>rd</sup> mode shows features in the northern and the southern of the SCS.



(a)



(b)



(c)

**Figure 4.15** The spatial patterns associated with their principal components of SSH in the SCS for: (a) mode 1, (b) mode 2 and (c) mode 3.

### 4.2.3 EOF of SSH from OCCAM with a resolution of $1/12^\circ$

The SSHs from OCCAM with resolution of  $1/12^\circ$  during February 1993 to January 2003 have 120 months. In this study, the data grids are considered only in the GoT with  $85 \times 97$  in space. The principal components of SSHs and their percentages of total variance for the GoT are shown in Figure 4.16. The first two modes of SSH account 98.50% with mode 1 and 2 explaining 89.32% and 9.18% of total variance, respectively. The first two spatial patterns associated with their principal components of SSH in the GoT are shown in Figure 4.17. The 1<sup>st</sup> mode of SSH represents the feature in the southern of the GoT. The 2<sup>nd</sup> mode shows the features in the central and the southern of the the GoT.

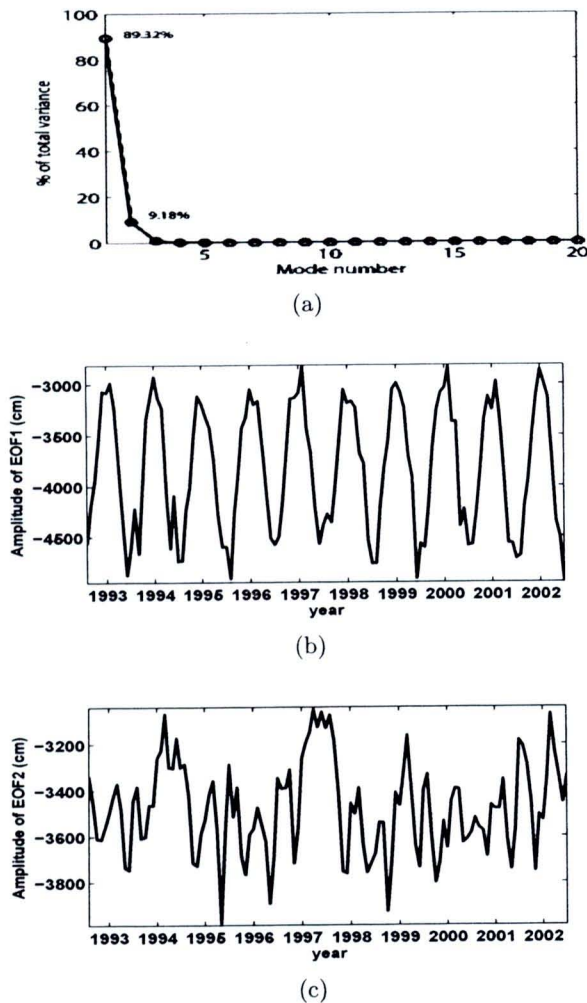
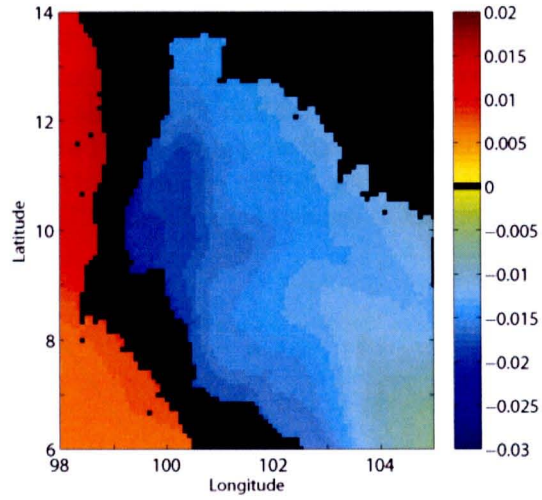
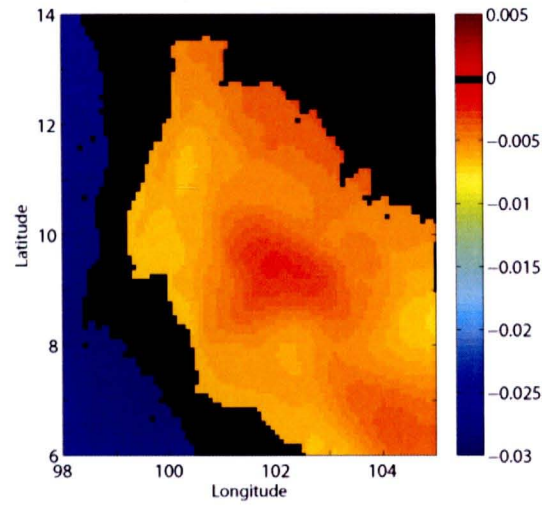


**Figure 4.16** EOF of SSH from OCCAM with a resolution of  $1/12^\circ$  during Feb 1993 to Jan 2003 in the GoT: (a) % of the total variance, (b) the principal components of SSH mode 1 and (c) the principal components of SSH mode 2.



(a)



(b)

**Figure 4.17** The spatial patterns associated with their principal components of SSH in the GoT for: (a) mode 1 and (b) mode 2.

For the SCS region, the data grids are  $217 \times 301$  in space for each time series. The EOFs can not calculate because of the grided data of SSH in this region are large in dimensions. The performance of computer can not compute the large data. So, the EOFs of SSH from OCCAM with a resolution of  $1/12^\circ$  in the SCS are not shown.

#### 4.2.4 EOF of SSH from POM

The monthly SSHs from POM are only investigated in the GoT. The SSH during February 1993 to January 2003 have 120 months with  $37 \times 97$  in space. Figure 4.18 shows the percentage of total variance and principal components of SSHs in the GoT. The first two modes of SSH in the GoT region account 89.05% with mode 1 and 2 explaining 76.45% and 12.60% of total variance, respectively. The two highest spatial patterns associated with their principal components of SSH in the GoT are shown in Figure 4.19. The 1<sup>st</sup> mode of SSH represents the features in the eastern and southern of the GoT. The 2<sup>nd</sup> mode shows the variation in the western along the coast of the GoT.

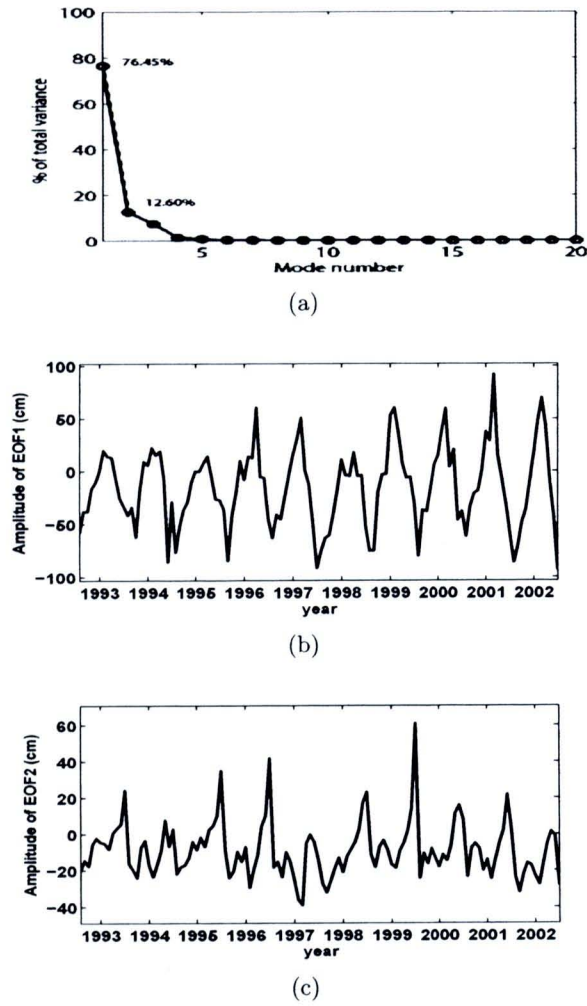
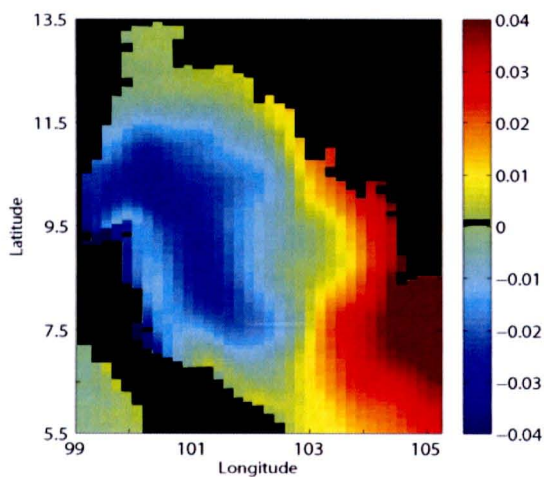
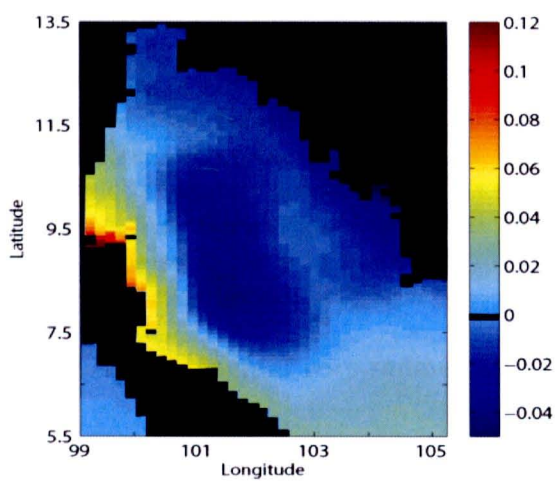


**Figure 4.18** EOF of SSH from POM during Feb 1993 to Jan 2003 in the GoT: (a) % of the total variance, (b) the principal components of SSH mode 1 and (c) the principal components of SSH mode 2.



(a)



(b)

**Figure 4.19** The spatial patterns associated with their principal components of SSH in the GoT for: (a) mode 1 and (b) mode 2.

In summary, the EOFs analysis of observation and results from numerical ocean models are analyzed. Four sources of grided data in the GoT, that is SSHA from TOPEX/ERS, SSH from OCCAM with a resolution of  $1/4^\circ$ , SSH from OCCAM with a resolution of  $1/12^\circ$  and SSH from POM have been analyzed. In the SCS, two sources of grided data such as SSHA from TOPEX/ERS and SSH from OCCAM with a resolution of  $1/4^\circ$  have been analyzed.

The EOFs of observation and results from numerical ocean models are shown in this chapter. Comparisons between EOFs of results from numerical ocean models in the GoT reveal that the first two modes of SSHs from OCCAM with resolutions of  $1/4^\circ$  and  $1/12^\circ$  are similarly features for each mode. They reveal significant feature in the southern of the GoT. They show the same pattern as of SSH from POM for the 1<sup>st</sup> mode, but in the 2<sup>nd</sup> modes of SSHs from OCCAM are not agree with the 2<sup>nd</sup> mode of SSH from POM. Comparisons between EOFs of observation and results from ocean models for each mode show that the first two modes of SSHA from TOPEX/ERS are different to the first two modes of SSHs from OCCAM with resolutions of  $1/4^\circ$  and  $1/12^\circ$ . Likewise, the first two modes of SSHA from TOPEX/ERS are different to the first two modes of SSHs from POM for each mode. In the SCS region, comparison between EOFs of SSHA from TOPEX/ERS and SSH from OCCAM with a resolution of  $1/4^\circ$  reveals that the first two modes of SSHA from TOPEX/ERS and SSH from OCCAM are different features but the 3<sup>rd</sup> modes of them are agree significant features in the northern and the southern of the SCS.

### 4.3 Wavelet Analysis

The wavelet analysis on principal components of SSHA from TOPEX/ERS, SSHs from OCCAM with resolutions of  $1/4^\circ$  and  $1/12^\circ$  and SSH from POM are analyzed in the GoT and the SCS during February 1993 to January 2003. Each panels of Figures 4.20 - 4.33 represent the principal component (panel a), wavelet power spectrum (panel b) and global wavelet spectrum (GWS) (panel c) for each mode. The black contours in panel b represent significant at the 5% level and black curve shows cone of influence. The solid curve in panel c is the GWS and dash line is significant at the 5% level for each period.

#### 4.3.1 Wavelet analysis on principal components of SSHA from TOPEX/ERS

The wavelet analysis on the first two modes principal components of SSHA from TOPEX/ERS in the GoT are shown in Figures 4.20 - 4.21 and the wavelet analysis of the first three modes principal components of SSHA from TOPEX/ERS in the SCS are shown in Figures 4.22 - 4.24.

The significant power in the spectrum of SSHA principal component mode 1 and its GWS in the GoT reveals the signals in Feb 1993 to Jan 2003 with period of 1 - 1.5 years (Figure 4.20). The wavelet power spectrum of SSHA principal component mode 2 and its GWS in the GoT is shown in Figure 4.21. The signal is observed in 1997 - 1998 with period of 1.5 - 4 years.

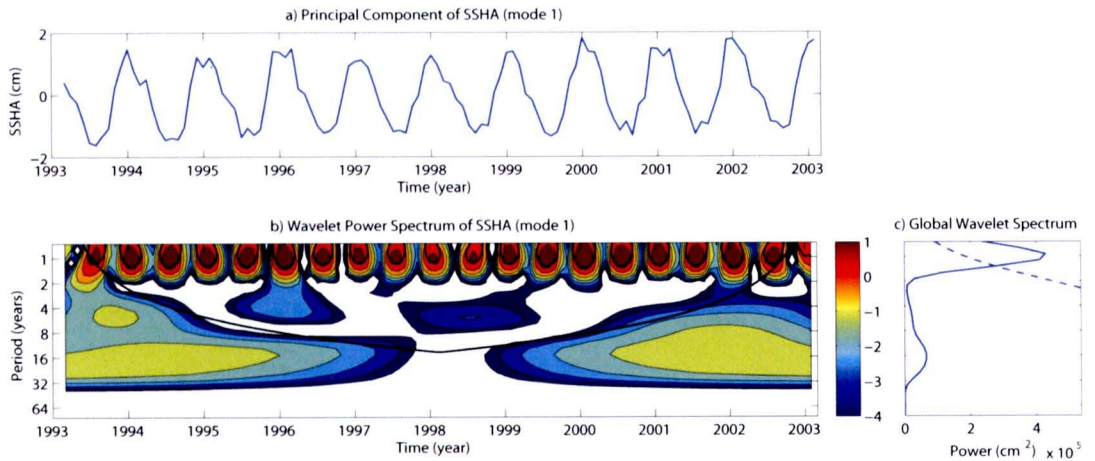


**Figure 4.20** The wavelet power spectrum of SSHA from TOPEX/ERS in GoT: (a) principal component of SSHA mode 1, (b) wavelet power spectrum of SSHA mode 1 along with cone of influence (black curve) and 95% confident interval (black contours), (c) global wavelet power spectrum (solid curve) and 95% confident interval (dash curve).

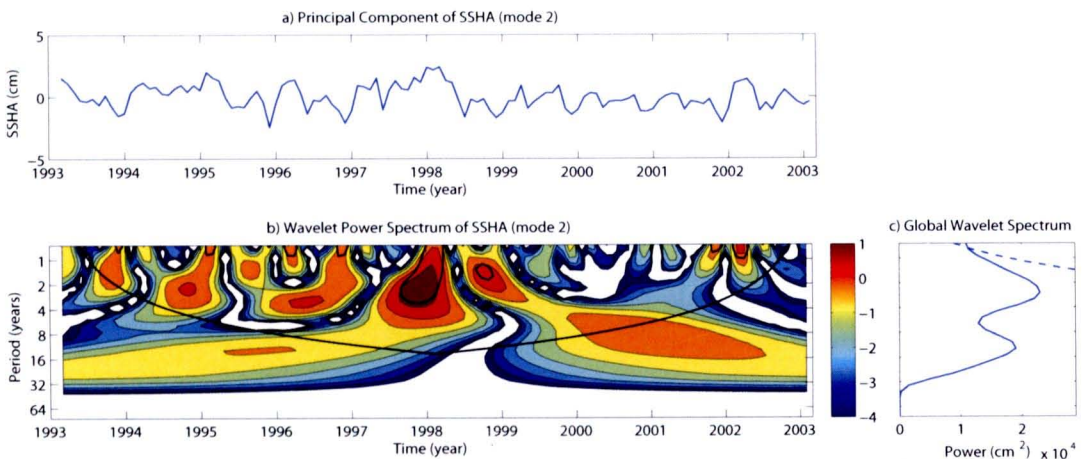


**Figure 4.21** Same as Figure 4.20 except for SSHA from TOPEX/ERS mode 2.

Figures 4.22 - 4.24 show the wavelet power spectrum and its GWS of SSHA from TOPEX/ERS in the SCS for the first three modes of principal components. The 1<sup>st</sup> mode of SSHA principal component represents signals which are the annual events on period of 1 - 1.5 years in Feb 1993 to Jan 2003, see Figure 4.22. The wavelet power spectrum of SSHA principal component mode 2 has signals in late 1997 - 1998 with period of 1.5 - 4 years and in late 1999 - 2000 with period of 6 - 10 years, as shown in Figure 4.23. Figure 4.24 shows signals in 1994 with period of 1 - 1.5 years, in 1997 with period of 1.5 - 3 years and in late 2001 - 2002 with period of 1 - 1.5 years.

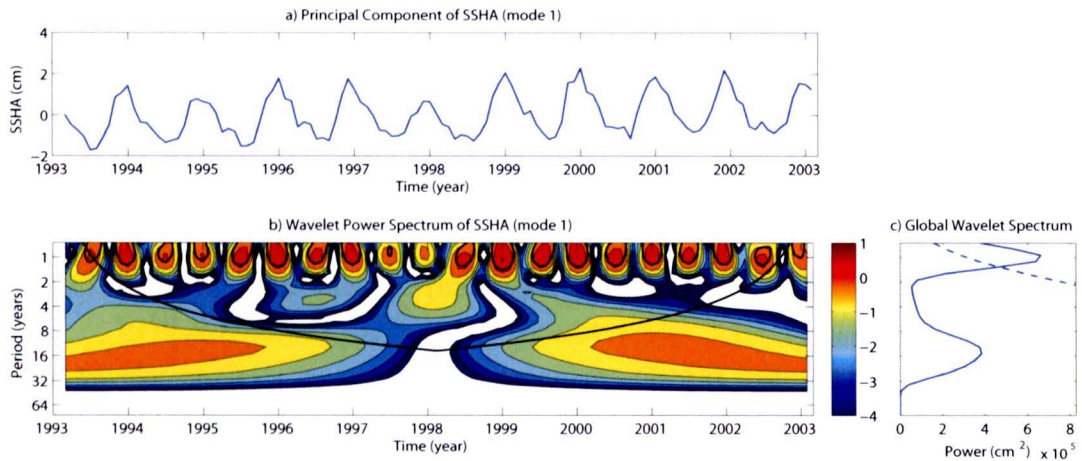


**Figure 4.22** The wavelet power spectrum of SSHA from TOPEX/ERS in SCS: (a) principal component of SSHA mode 1, (b) wavelet power spectrum of SSHA mode 1 along with cone of influence (black curve) and 95% confident interval (black contours), (c) global wavelet power spectrum (solid curve) and 95% confident interval (dash curve).

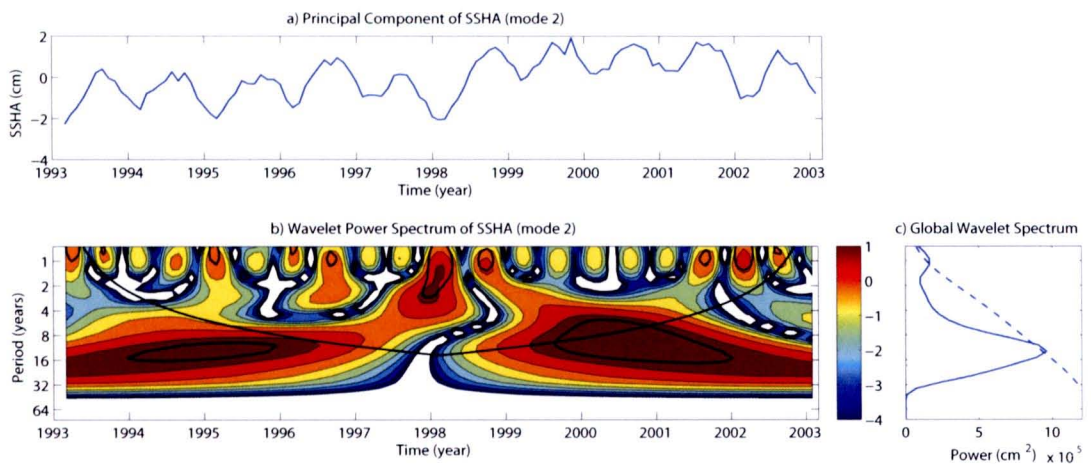


**Figure 4.23** Same as Figure 4.22 except for SSHA from TOPEX/ERS mode 2.

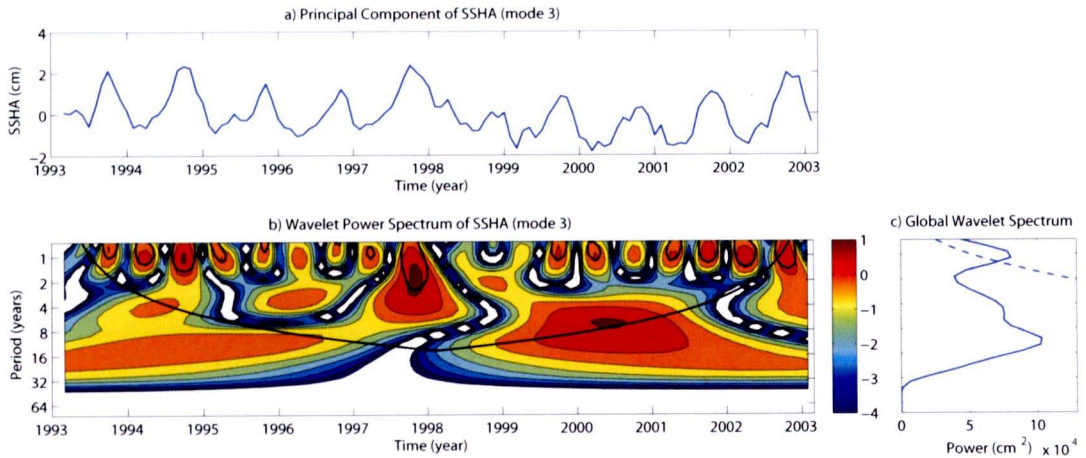


**Figure 4.24** Same as Figure 4.22 except for SSHA from TOPEX/ERS mode 3.

#### 4.3.2 Wavelet analysis on principal components of SSH from OCCAM with a resolution of $1/4^\circ$

The wavelet analysis on principal components of SSH from OCCAM with a resolution of  $1/4^\circ$  in the GoT and the SCS are shown in Figures 4.25 - 4.29. There are wavelet analysis of the first two modes and the first three modes of principal components of SSH in the GoT and the SCS, respectively.

The wavelet power spectrum of SSH from OCCAM with a resolution of  $1/4^\circ$  in the GoT and its GWS of principal component mode 1 are shown in Figure 4.25. This figure reveals the annual signals in Feb 1993 to Jan 2003 with period of 1 - 1.5 years. Figure 4.26 shows the wavelet power spectrum of SSH and its GWS of principal component mode 2 which represents signal in 1997 - 1998 with period of 1 - 4 years.

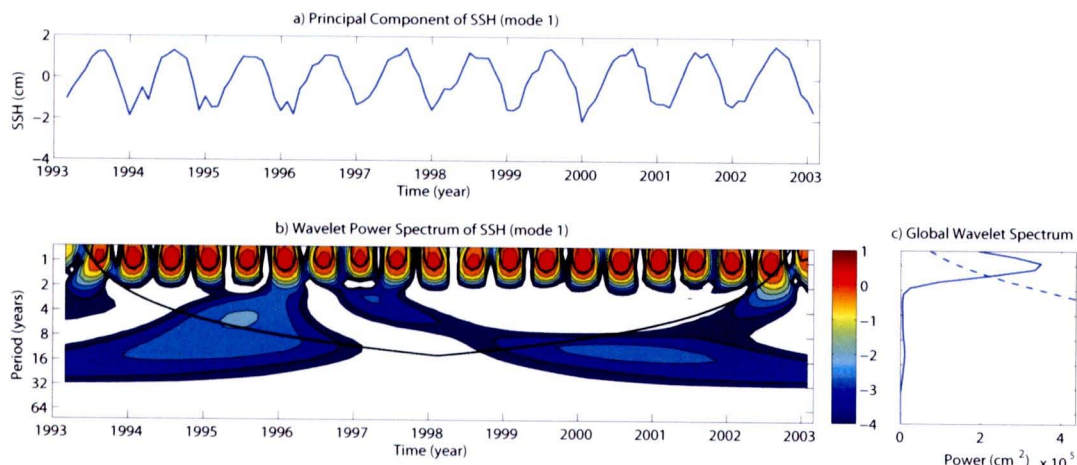


**Figure 4.25** The wavelet power spectrum of SSH from OCCAM with a resolution of  $1/4^\circ$  in GoT: (a) principal component of SSH mode 1, (b) wavelet power spectrum of SSH mode 1 along with cone of influence (black curve) and 95% confident interval (black contours), (c) global wavelet power spectrum (solid curve) and 95% confident interval (dash curve).

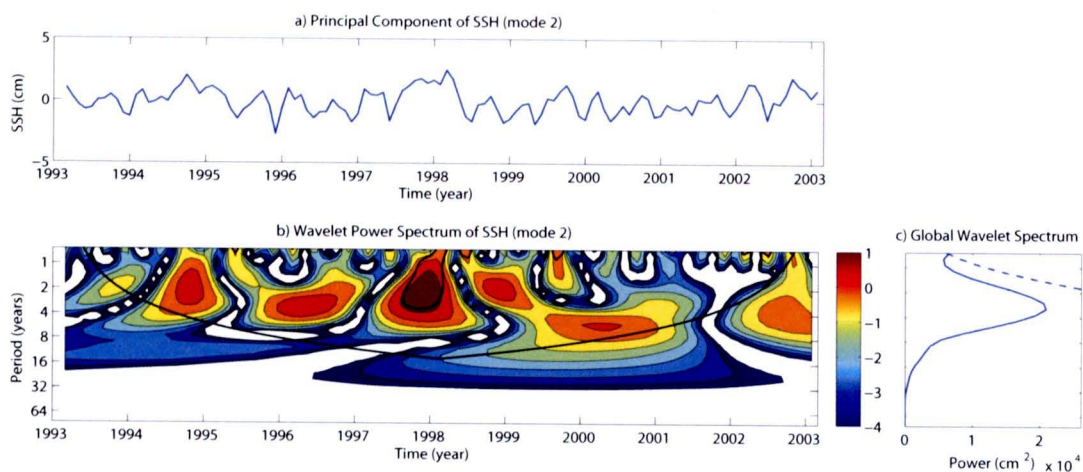


**Figure 4.26** Same as Figure 4.25 except for SSH from OCCAM with a resolution of  $1/4^\circ$  mode 2.

Figure 4.27 represents the wavelet power spectrum of SSH from OCCAM model with a resolution of  $1/4^\circ$  in the SCS and its GWS of principal component mode 1. The signals reveal on period of 1 - 1.5 years in Feb 1993 to Jan 2003. For the 2<sup>nd</sup> mode, the wavelet power spectrum of SSH and its GWS reveal signals in late 1997 - 1998 with period of 1 - 4 years, see Figure 4.28. The wavelet power spectrum of SSH principal component mode 3, as shown in Figure 4.29, observed signals in late 1997 - 1998 with period of 1 - 4 years.

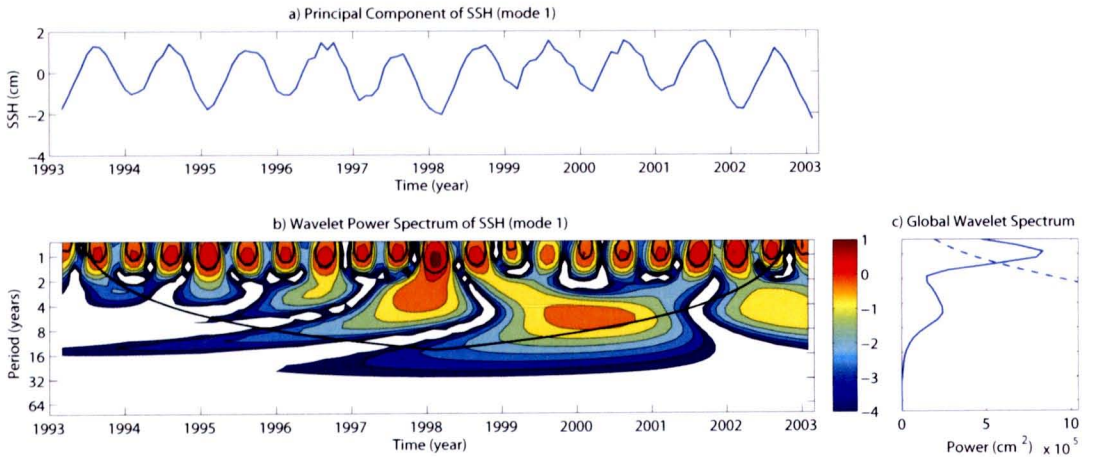


**Figure 4.27** The wavelet power spectrum of SSH from OCCAM with a resolution of  $1/4^\circ$  in SCS: (a) principal component of SSH mode 1, (b) wavelet power spectrum of SSH mode 1 along with cone of influence (black curve) and 95% confident interval (black contours), (c) global wavelet power spectrum (solid curve) and 95% confident interval (dash curve).

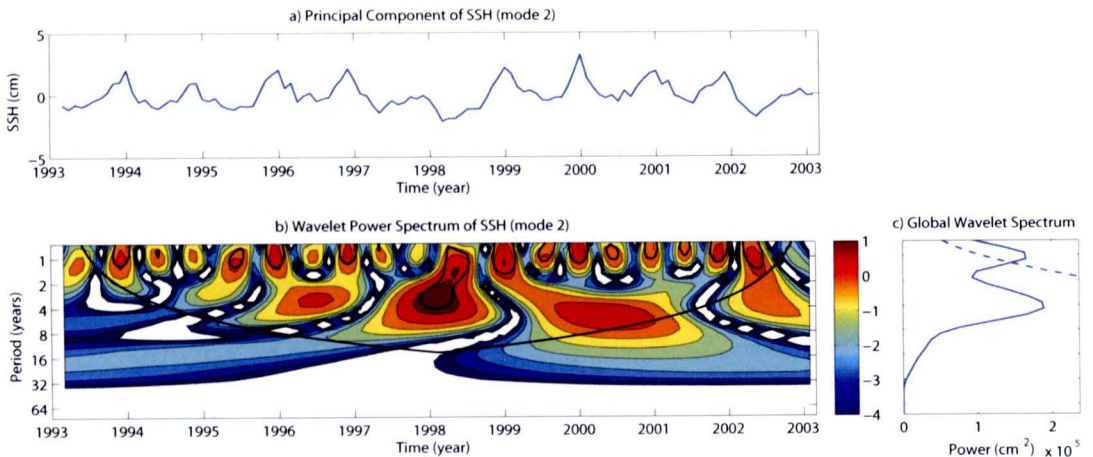


**Figure 4.28** Same as Figure 4.27 except for SSH from OCCAM with a resolution of  $1/4^\circ$  mode 2.

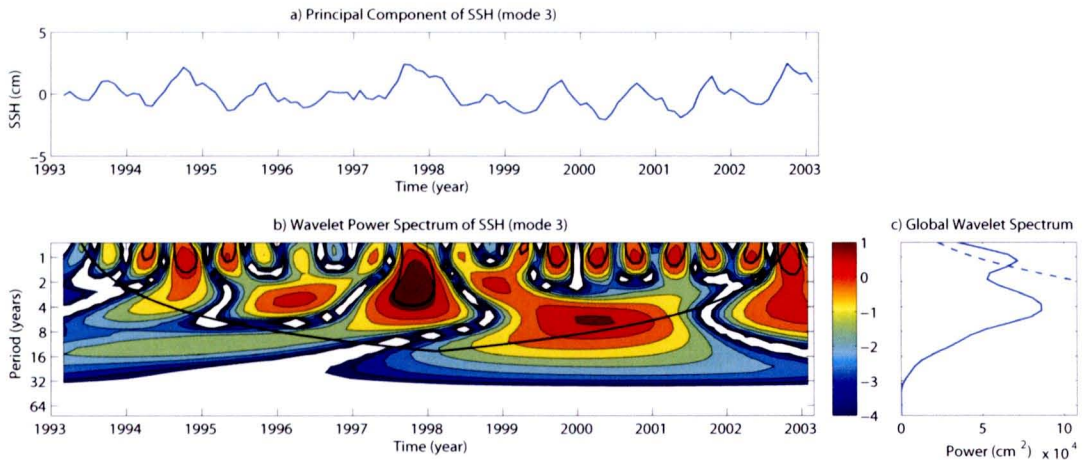


**Figure 4.29** Same as Figure 4.27 except for SSH from OCCAM with a resolution of  $1/4^\circ$  mode 3.

#### 4.3.3 Wavelet analysis on principal components of SSH from OCCAM with a resolution of $1/12^\circ$

The wavelet analysis on the first two modes principal components of SSH from OCCAM with a resolution of  $1/12^\circ$  in the GoT are shown in Figures 4.30 - 4.31. The significant power in the spectrum of SSH from OCCAM with a resolution of  $1/12^\circ$  for principal component mode 1 in the GoT reveals the annual signals in Feb 1993 to Jan 2003 with period of 1 - 1.5 years, see Figure 4.30. The wavelet power spectrum of SSHA principal component mode 2 in the GoT and its GWS are shown in Figure 4.31. The signal is found in late 1997 - 1998 with period of 1 - 4 years.

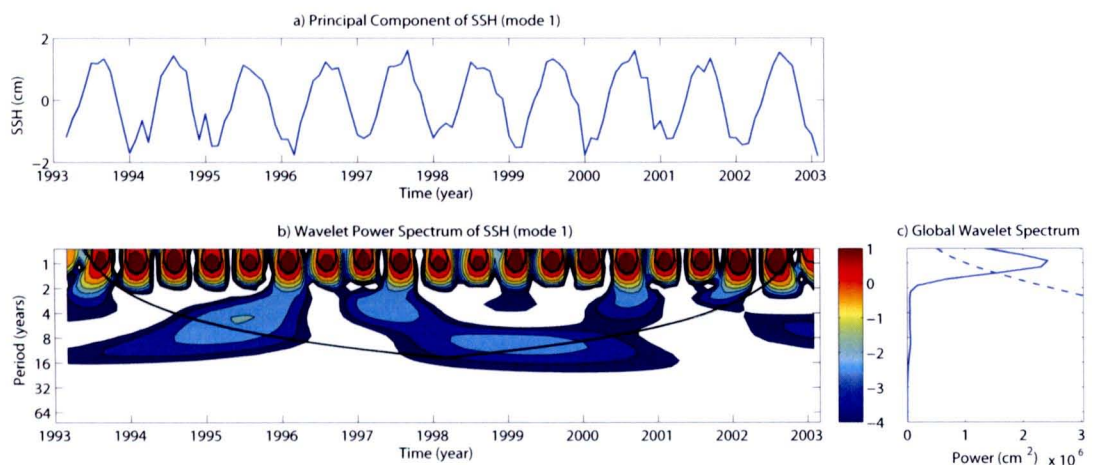


**Figure 4.30** The wavelet power spectrum of SSH from OCCAM with a resolution of  $1/12^\circ$  in GoT: (a) principal component of SSH mode 1, (b) wavelet power spectrum of SSH mode 1 along with cone of influence (black curve) and 95% confident interval (black contours), (c) global wavelet power spectrum (solid curve) and 95% confident interval (dash curve).

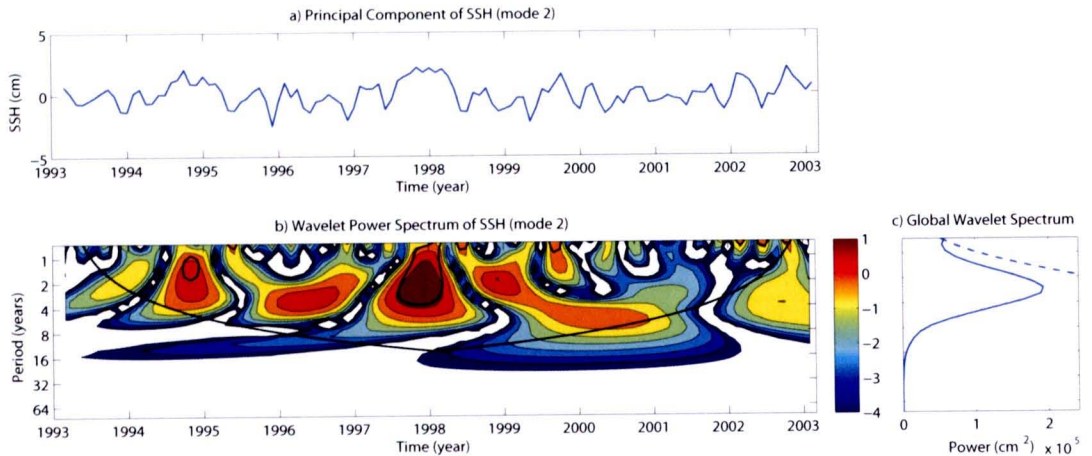


**Figure 4.31** Same as Figure 4.30 except for SSH from OCCAM with a resolution of  $1/12^\circ$  mode 2.

#### 4.3.4 Wavelet analysis on principal components of SSH from POM

The wavelet analysis on the first two modes principal components of SSH from POM in the GoT are shown in Figures 4.32 - 4.33. The significant power in the spectrum of SSH principal component mode 1 and its GWS in the GoT reveals the annual signals in late 1994 - 2002 with period of 1 - 1.5 years (Figure 4.32). The wavelet power spectrum of SSH principal component mode 2 and its GWS is shown in Figure 4.33. The signals are observed in 1997 and 2000 with period of 1 - 1.5 years.

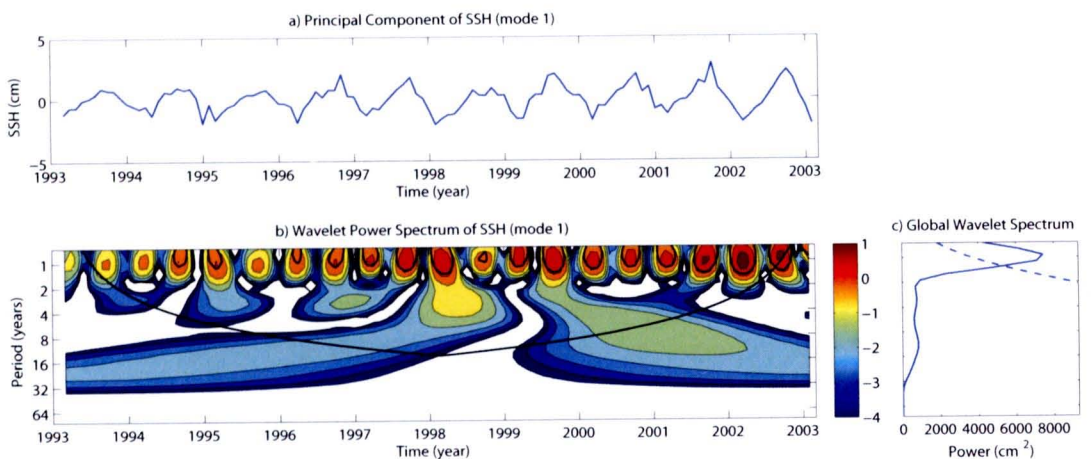


**Figure 4.32** The wavelet power spectrum of SSH from POM in GoT: (a) principal component of SSH mode 1, (b) wavelet power spectrum of SSH mode 1 along with cone of influence (black curve) and 95% confident interval (black contours), (c) global wavelet power spectrum (solid curve) and 95% confident interval (dash curve).

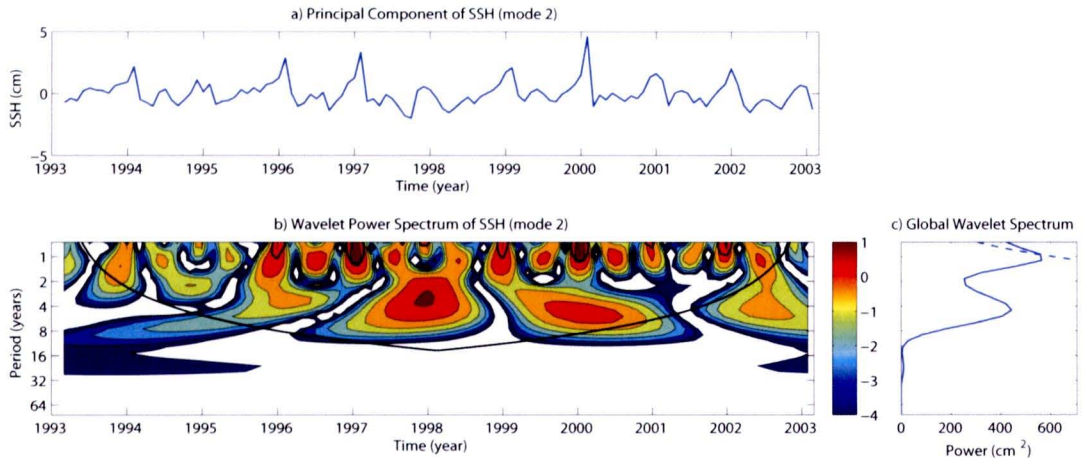


**Figure 4.33** Same as Figure 4.32 except for SSH from POM mode 2.

In summary, the results from wavelet analysis supported the EOF analysis. The principal components of SSHA from TOPEX/ERS and SSH from numerical ocean models in the GoT and the SCS are further investigate using the wavelet power spectrum for each mode. In the GoT, the annual signals of SSHs mode 1 from OCCAM model with resolutions of  $1/4^\circ$  and  $1/12^\circ$  are observed in February 1993 - January 2003 with period of 1 - 1.5 years. They are similarly to signals of SSHA mode 1 from TOPEX/ERS. Especially, the wavelet power spectrum of SSHA from TOPEX/ERS are high power as wavelet power spectrum of SSH from OCCAM with a resolution of  $1/12^\circ$ . The wavelet power spectrum of SSH mode 1 from POM are lower power than them in late 1994 - 2002 with period of 1 - 1.5 years. The 2<sup>nd</sup> mode of wavelet power spectrum of SSHA from TOPEX/ERS and SSHs from OCCAM with resolutions of  $1/4^\circ$  and  $1/12^\circ$  have similarly signal in late 1997 - 1998 with period of 1.5 - 4 years while the 2<sup>nd</sup> mode of wavelet power spectrum of SSH from POM has signals in 1997 and 2000 with period 1 - 1.5 years. In the SCS, the wavelet power spectrum of SSHA from TOPEX/ERS and SSH from OCCAM with a resolution of  $1/4^\circ$  are investigated. The 1<sup>st</sup> mode, the annual signals of SSHA from TOPEX/ERS and SSH from OCCAM are found in February 1993 - January 2003 with period of 1 - 1.5 years. The wavelet power spectrum of both data have same signal in late 1997 - 1998 but the wavelet power spectrum of SSH from OCCAM has longer period more than the wavelet power spectrum of SSHA from TOPEX/ERS for the 2<sup>nd</sup> and the 3<sup>rd</sup> modes.

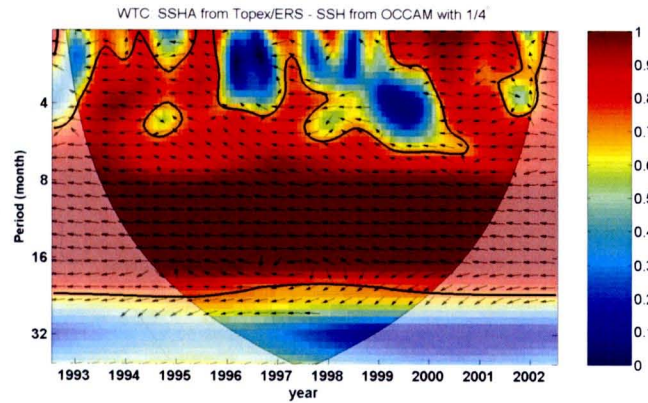
## 4.4 Wavelet Coherence

The wavelet coherence is used to investigate relationships between two time series. The significance level of the wavelet coherence is estimated by Monte Carlo methods. The wavelet coherence gives a quantity between 0 and 1 (Torrence and Compo, 1998). Vectors in figures indicate the phase different between two time series. There are in-phase, anti-phase, time series 1 leading time series 2 by  $90^\circ$  and time series 2 leading time series 1 by  $90^\circ$  if vectors indicate in the right, left, down and up directions, respectively. Comparison between principal components of the observation and results from numerical ocean models in the GoT and the SCS during February 1993 to January 2003 are discussed in this study.

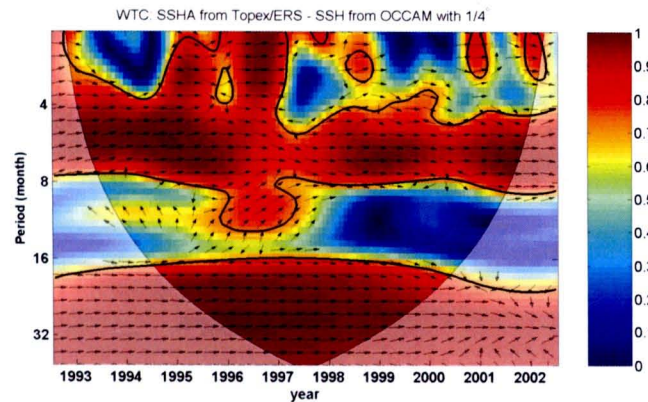
### 4.4.1 Wavelet coherence on principal components of SSHA from TOPEX/ERS and SSH from OCCAM with a resolution of $1/4^\circ$

The principal components of SSHA from TOPEX/ERS and SSH from OCCAM with a resolution of  $1/4^\circ$  are used to find the relations in the GoT and the SCS. The correlations between principal components mode 1 of SSHA and SSH in the GoT, as shown in Figure 4.34(a). The figure reveals that highly coherence which is anti-phase variations occurs in 1994 - 2001 with period of 8 - 16 months and in late 2000 - 2001 with period of 1 - 2 months. Figure 4.34(b) shows the relations between principal components mode 2 of SSHA and SSH in the GoT. The figure represents the coherence occurs in late 1993 - 1996 with period of 5 - 7 months, in 1997 with period of 1 - 3 months, in 1998 - 2000 and 2001 with period of 6 - 7 months and in 1995 - 2000 with period of 24 - 48 months. These areas show in-phase variations between principal components of SSHA and SSH in the GoT.

In the SCS, the correlations between principal components mode 1 of SSHA from TOPEX/ERS and SSH from OCCAM with a resolution of  $1/4^\circ$  is shown in Figure 4.35(a). The coherence occurs in 1995 - 1996 with period of 4 - 7 months and in late 1995 - 2000 with period of 24 - 32 months, which the SSH lead SSHA by 0.5 - 1 month and 2.3 - 4.7 months, respectively. In the period of 10 - 14 months, the SSH lead SSHA by 4.5 months during 1994 - 1997 and 1999 - 2001. Figure 4.35(b) reveals the coherence between principal component mode 2 of SSHA and SSH. This figure shows the coherence between SSHA and SSH in 1994 - 1996 with period of 10 - 14 months, which SSH lead SSHA by 3 months. In period of 5 - 7 months, the coherence is in-phase relationship. Figure 4.35(c) shows the relationship of SSHA and SSH principal component mode 3. The highly coherence occur in 1994 - 1996 and 1999 - 2001 with period of 10 - 14 months and in 1996 - 1998 with period of 20 - 48 months. The correlations of SSHA and SSH are in-phase variations for each time and each period.

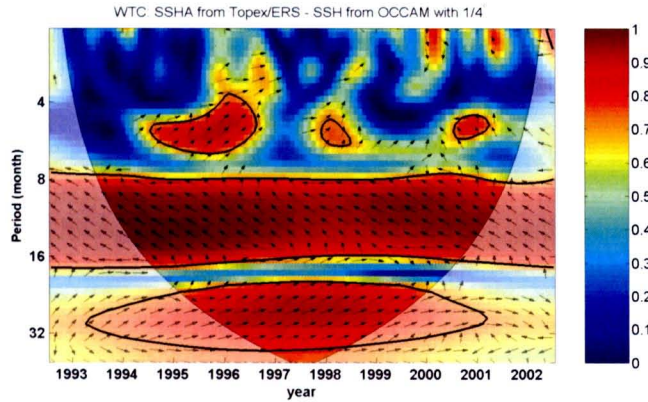


(a)

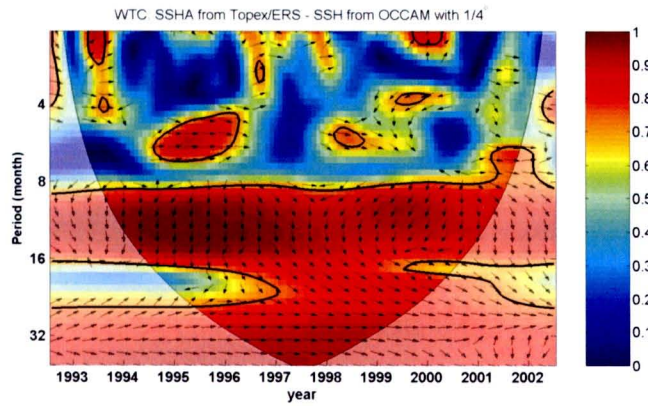


(b)

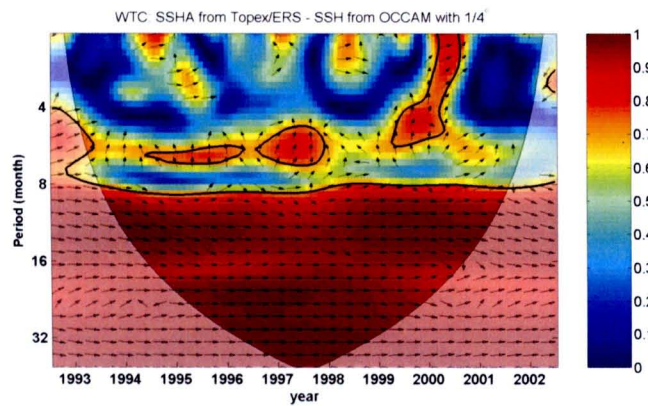
**Figure 4.34** The wavelet coherence and phase relationship between SSHA from TOPEX/ERS and SSH from OCCAM with a resolution of  $1/4^\circ$  in the GoT during Feb 1993 - Jan 2003 with the 5% significance level (thick black contour) and the cone of influence using: (a) principal components mode 1 and (b) principal components mode 2.



(a)



(b)

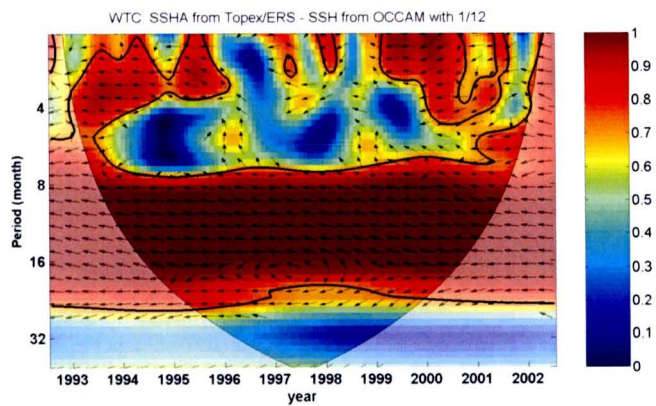


(c)

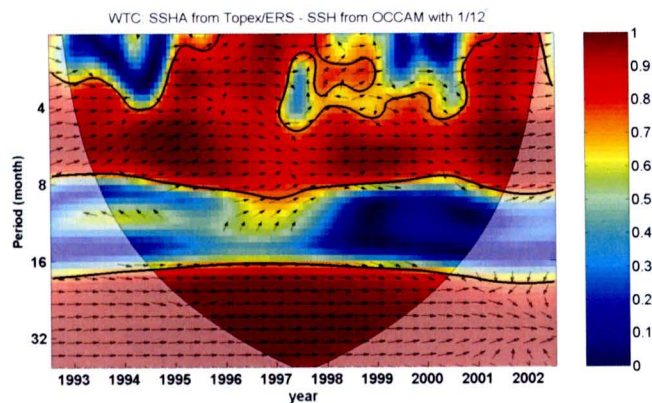
**Figure 4.35** Same as Figure 4.34 but except for the SCS using: (a) principal components mode 1, (b) principal components mode 2 and (c) principal components mode 3.

#### 4.4.2 Wavelet coherence on principal components of SSHA from TOPEX/ERS and SSH from OCCAM with a resolution of $1/12^\circ$

The principal components of SSHA from TOPEX/ERS and SSH from OCCAM with a resolution of  $1/12^\circ$  are investigated the relationship in the GoT. The correlations between principal components mode 1 of SSHA and SSH are shown in Figure 4.36(a). The figure represents highly coherence with anti-phase variations occurs in 1994 - 2001 with period of 8 - 16 months and in late 1999 - 2000 with period of 1 - 3 months. Figure 4.36(b) shows the relations between principal components mode 2 of SSHA and SSH. The coherence occurs in 1994 - 1996 and 2001 with period of 5 - 7 months, the SSH lead SSHA by 0.5 month. The coherence with in-phase variations occurs in 1995 - 2000 with period of 20 - 48 months.



(a)

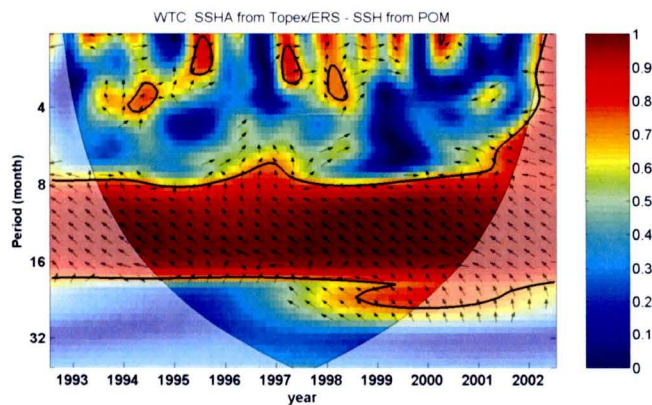


(b)

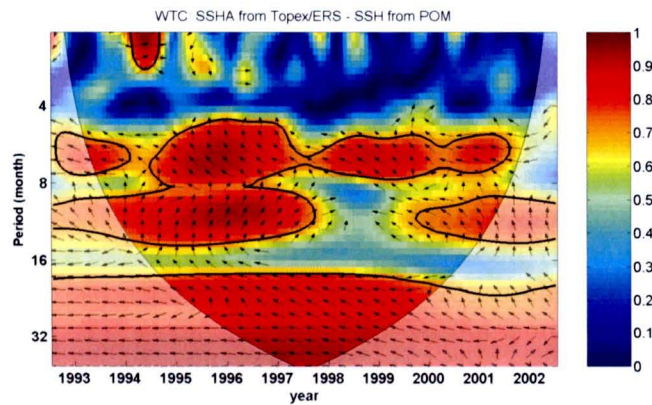
**Figure 4.36** The wavelet coherence and phase relationship between SSHA from TOPEX/ERS and SSH from OCCAM with a resolution of  $1/12^\circ$  in the GoT during Feb 1993 - Jan 2003 with the 5% significance level (thick black contour) and the cone of influence using: (a) principal components mode 1 and (b) principal components mode 2.

#### 4.4.3 Wavelet coherence on principal components of SSHA from TOPEX/ERS and SSH from POM

The principal components of SSHA from TOPEX/ERS and SSH from POM are investigated the correlation in the GoT. The relations between principal components mode 1 of SSHA and SSH are shown in Figure 4.37(a). The figure reveals coherence occurs in 1994 - 2001 with period of 10 - 14 months which the SSH lead SSHA by 4.5 months. Figure 4.37(b) shows the relations between principal components mode 2 of SSHA and SSH. The coherence with in-phase occurs in late 1994 with period of 1 - 2 months. In 1995 - 1996 with period of 6 - 8 months, the SSH lead SSHA by 2.6 months. In 1996 - 1997 with period of 10 - 14 months, the SSH lead SSHA by 2 months. The coherence is anti-phase variations in 1997 - 1998 with period of 32 - 48 months.



(a)



(b)

**Figure 4.37** The wavelet coherence and phase relationship between SSHA from TOPEX/ERS and SSH from POM in the GoT during Feb 1993 - Jan 2003 with the 5% significance level (thick black contour) and the cone of influence using: (a) principal components mode 1 and (b) principal components mode 2.

The wavelet coherence is used to analyze the relationships between principal components of the observation and results from numerical models in the GoT and the SCS during February 1993 to January 2003. There are principal components of SSHA from TOPEX/ERS, SSHs from OCCAM with resolutions of  $1/4^\circ$  and  $1/12^\circ$  and SSH from POM. The first two modes of principal components of all data sets are investigated in the GoT but only the first three modes of SSHA from TOPEX/ERS and SSH from OCCAM with a resolution of  $1/4^\circ$  are investigated in the SCS.

Tables 4.2 - 4.3 reveal the relationships between principal components of SSHA from TOPEX/ERS and SSH from numerical ocean models for each mode in the GoT and the SCS. Each column represents SSH from numerical ocean models while each row represents dominant mode. The negative sign means SSHA from TOPEX/ERS lag SSH from numerical ocean model.

**Table 4.2** The relationships between SSHA from TOPEX/ERS and SSH from numerical ocean models for each mode in the GoT

	OCCAM $1/4^\circ$	OCCAM $1/12^\circ$	POM
<b>Mode 1</b>	anti-phase	anti-phase	- 4.5 months
<b>Mode 2</b>	in-phase	in-phase	- 2 months

**Table 4.3** Same as Table 4.2 except for the SCS

	OCCAM $1/4^\circ$
<b>Mode 1</b>	- 4.5 months
<b>Mode 2</b>	- 3 months
<b>Mode 3</b>	in-phase

In the GoT, the relations for each mode of principal components of SSHA from TOPEX/ERS and SSH from OCCAM with a resolution of  $1/4^\circ$  are likely behavior as relations between principal components of SSHA from TOPEX/ERS and SSH from OCCAM with a resolution of  $1/12^\circ$ . The 1<sup>st</sup> mode, the high coherence is anti-phase variations in 1994 - 2001 with period of 8 - 16 months and in 2001 with period of 1 - 2 months. The 2<sup>nd</sup> mode, the high relationship is in-phase variations in 1997 with period of 1 - 3 months, in 1998 - 2000 and 2001 with period of 6 - 7 months and in 1995 - 2000 with period of 24 - 48 months. The relation of SSHA from TOPEX/ERS and SSH from OCCAM with a resolution of  $1/4^\circ$  is in-phase but the coherence of SSHA from TOPEX/ERS lag SSH from OCCAM with a resolution of  $1/12^\circ$  by approximately 0.5 month in late 1993 - 1996 with period of 5 - 7 months. The relationships between the first two modes principal components of SSHA from TOPEX/ERS and SSH from POM are not likely behavior with relations of SSHA from TOPEX/ERS and SSHs from OCCAM. The high coherence of the 1<sup>st</sup> mode of SSHA from TOPEX/ERS and SSH from POM occurs in 1994 - 2001 with period of 10 - 14 months which SSHA lag SSH by approximately 4.5 months. The 2<sup>nd</sup> mode, the coherence which are in-phase relationship occur in late 1994 with period of 1 - 2 months and in 1997 - 1998 with period of 32 - 48 months. The SSHA lag SSH by approximately 2 months in 1996 - 1997 with period of 10 - 14 months.

In the SCS, the relationships between principal components of SSHA from TOPEX/ERS and SSH from OCCAM with the resolution of  $1/4^\circ$  are analyzed. The 1<sup>st</sup> mode, the coherence occurs in 1995 - 1996 with period of 4 - 7 months and in late 1995 - 2000 with period of 24 - 32 months, which the SSHA lag SSH by 0.5 - 1 month and 2.3 - 4.7 months, respectively. In the period of 10 - 14 months, the SSHA lag SSH by approximately 4.5 months during 1994 - 1997 and 1999 - 2001. The 2<sup>nd</sup> mode, the coherence between SSHA and SSH in 1994 - 1996 with period of 10 - 14 months, which SSHA lag SSH by 3 months. In period of 5 - 7 months, the coherence is in-phase relationship during 1996 - 1999. The 3<sup>rd</sup> mode, the high coherence occur in 1994 - 1996 and 1999 - 2001 with period of 10 - 14 months and in 1996 - 1998 with period of 20 - 48 months. The correlations of SSHA and SSH are in-phase variations for each time and each period.